control). Mice were killed at 6, 24, or 168 hours after administration for flow cytometric analysis. Experiment 9 (Figure 6): Immunosufficient C57BL/6 mice were administered with splenic CD4+ T cells from CAG-GFP Tg mice intrarectally (B6-IR mice; 1×10^7 cells) or intravenously (B6-IV mice; 1×10^6 cells, as a control). Mice were killed at 6, 24, or 168 hours after administration for flow cytometric analysis. Experiment 10 (Supplementary Figure 6): C57BL/6-background RAG-$2^{-/-}$ mice were administered with splenic CD4+ T cells from CAG-GFP Tg mice intrarectally (1×10^7) or intraperitoneally (1×10^6, as a control). Mice were killed at 10 weeks after administration for flow cytometric analysis. Experiment 11 (Supplementary Figure 7): RAG-$2^{-/-}$ or lymphotoxin α-deficient × RAG-$2^{-/-}$ mice were administered with splenic CD4+ T cells from CAG-GFP Tg mice intrarectally (1×10^7). Mice were killed at 14 days after administration. Experiment 12 (Figure 7*A* and *B*): RAG-$2^{-/-}$ mice were intrarectally administered with 1×10^7 splenic CD4+ T cells obtained from wild-type C57BL/6 or age-matched CCR$7^{-/-}$ mice and were killed at 14 days after administration. Experiment 13 (Figure 7*C* and *D*): RAG-$2^{-/-}$ mice were pretreated with PBS or FTY720 (1.0 mg/kg) daily starting 1 day before the transfer over a period of 2 weeks and were administered with 3×10^6 CD4+ T cells from CAG-GFP Tg mice intrarectally (1×10^7). Mice were killed at 14 days after administration.

Immunohistochemistry

For mice studies, tissue samples were fixed in PBS containing 10% neutral-buffered formalin. Paraffin-embedded sections (5 mm) were stained with H&E. The sections were analyzed without prior knowledge of the type of T-cell reconstitution or recipient. The area most affected was graded by the number and severity of lesions. The mean degree of inflammation in the colon was calculated using a modification of a previously described scoring system.[1-3] Consecutive cryostat colon sections were used for immunohistochemistry with purified hamster mAb against CD3e (BD PharMingen, San Diego, CA) and rabbit polyclonal Ab against cytokeratine (DAKO, Glostrup, Denmark). Briefly, Optimal cutting temperature (O.C.T.) compound-embedded tissue samples were cut into serial sections 6 mm thick, placed on coated slides, and fixed with 4% paraformaldehyde phosphate buffer solution for 30 minutes. Slides were then incubated with the primary antibody at 4°C for overnight then stained with Alexa Fluor 594 goat anti-hamster immunoglobulin G (Invitrogen, San Diego, CA) for CD3e detection and with Alexa Fluor 488 donkey anti-rabbit immunoglobulin G for cytokeratine detection at room temperature for 60 minutes. All slides were counterstained with 4′, 6′-diamidino-2-phenylindole (DAPI; Vector Laboratories, Burlingame, CA) and observed under a confocal microscope (LSM510; Carl Zeiss, Jena, Germany). For human studies, sections (4 mm thick) of the colons and rectums were fixed in 10% buffered formalin and processed for routine pathologic examination. Two paraffin-embedded tissue blocks that included the most crypt abscesses were selected in each case and used for the study. The staining conditions are described in Supplementary Table 2.

Electron Microscopy

The colons of the mice were cut into 1-mm pieces and fixed in 2.5% glutaraldehyde and embedded in Epon. Ultrathin sections (95 nm thick) were cut on a Reichert Ultracut S (Leica Microsystems; Heidelberg GmbH, Mannheim, Germany) and collected on Maxtaform grids (Pyser-SGL Ltd, Kent, UK). The sections were double stained with uranyl acetate and lead citrate and examined with an H-7100 electron microscope (Hitachi High-Technologies Co, Tokyo, Japan).[4]

Flow Cytometry

To detect the surface expression of a variety of molecules, isolated spleen, mesenteric lymph node (MLN), or LP mononuclear cells were preincubated with an Fc gamma II/III receptor-blocking mAb (CD16/32; 2.4G2; BD PharMingen) for 15 minutes then incubated with specific FITC-, PE-, PerCP-, allophycocyanin- or biotin-labeled antibodies for 20 minutes on ice. Biotinylated antibodies were detected with PE-streptavidin. Standard 3- or 4-color flow cytometric analyses were obtained using the FACS Calibur with CellQuest software. Background fluorescence was assessed by staining with control-irrelevant isotype-matched mAbs.

Statistical Analysis

First, we examined the normality of each group If either of 2 groups was not normally distributed, we assessed the difference between the 2 groups, with the Mann–Whitney *U* test. If both groups were normally distributed, we assessed the variance of population to which each group belonged with the *F* test. With homoscedasticity of both populations, we assessed the difference between 2 groups, using the Student *t* test. Without homoscedasticity, we assessed the difference with the Welch *t* test. We used the program Statcell (OMS Ltd Tokorozawa, Saitama, Japan) for all statistical analysis. The results were expressed as the mean ± standard error of the mean. Differences were considered to be statistically significant when $P < .05$.

References

1. Makita S, Kanai T, Nemoto Y, et al. Intestinal lamina propria retaining CD4+CD25+ regulatory T cells is a suppressive site of intestinal inflammation. J Immunol 2007;178:4937–4946.
2. Totsuka T, Kanai T, Nemoto Y, et al. IL-7 is essential for the development and the persistence of chronic colitis. J Immunol 2007;178:4737–4748.
3. Nemoto Y, Kanai T, Makita S, et al. Bone marrow retaining colitogenic CD4+ T cells may be a pathogenic reservoir for chronic colitis. Gastroenterology 2007;132:176–189.
4. Ito T, Kobayashi D, Uchida K, et al. *Helicobacter pylori* invades the gastric mucosa and translocates to the gastric lymph nodes. Lab Invest 2008;88:664–681.

Supplementary Table 1. Patients Enrolled in the Study

No.	Sex	Age, *y*	Pathologic diagnosis
UC1	Male	69	Ulcerative colitis, active phase of the colon and rectum
UC2	Male	68	Ulcerative colitis with toxic megacolon
UC3	Male	29	Adenocarcinoma of the descending colon. Ulcerative colitis
UC4	Male	53	Advanced rectal cancer. Ulcerative colitis

-Pre-medication

1, Give recipient mice 1ml of Niflec® (Ajinomoto Pharma Co., Tokyo), which is an oral bowel cleaner for human, at the concentration of 69g/L (standard concentration for human) three times at intervals of 1 hour, using oral catheter.
2, Stop any feed except water for recipient mice.

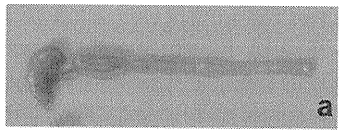

a. Gross appearance of the colon at day 2, after the pre-medication with Niflec®.

3, Six hours after the administration of Niflec®, insert the anal catheter into the colon of recipient mice to the depth of 3cm, and give 100μl 50% Ethanol through the catheter.
4, One hour after administration of Ethanol, 100μl 5% pronase (kaken Pharmaceutical Co., Ltd., Tokyo) was given to mice intrarectally as mentioned above.

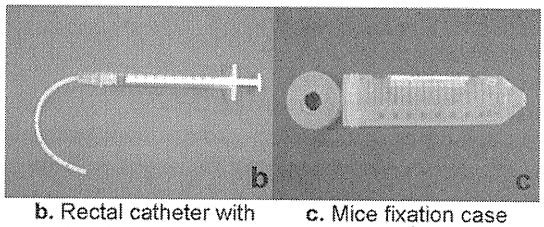

b. Rectal catheter with 1ml syringe

c. Mice fixation case

-Cell transfer

1, One hour after the pre-medication, insert the anal catheter into colon of recipient mice to the depth of 3cm (**d**), and give cells suspended to 200μl PBS. Reduce the defluvium using tweezers (**e**).
2, Shut the anal of recipient mice with the adhesive (**f**).

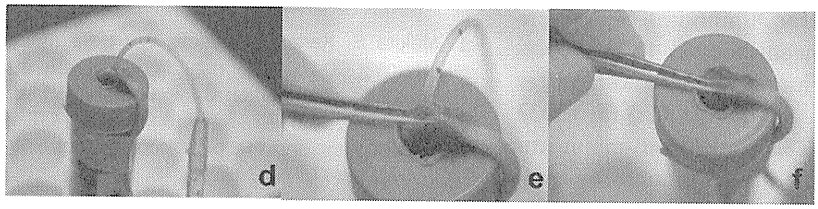

3, Six hours after the cell transfer, remove the adhesive from every mice.
4, Start feeding.

Supplementary Figure 1. Procedure of intrarectal administration of $CD4^+$ T cells into mice (*a*) Gross appearance of colon 6 after Niflec treatment. (*b*) Catheter with 1-mL syringe for pronase and ethanol treatment and intrarectal administration. (*c*) Mice fixation case. This device is made from a 50-mL Falcon tube. (*d–f*) Procedures for intrarectal cell administration.

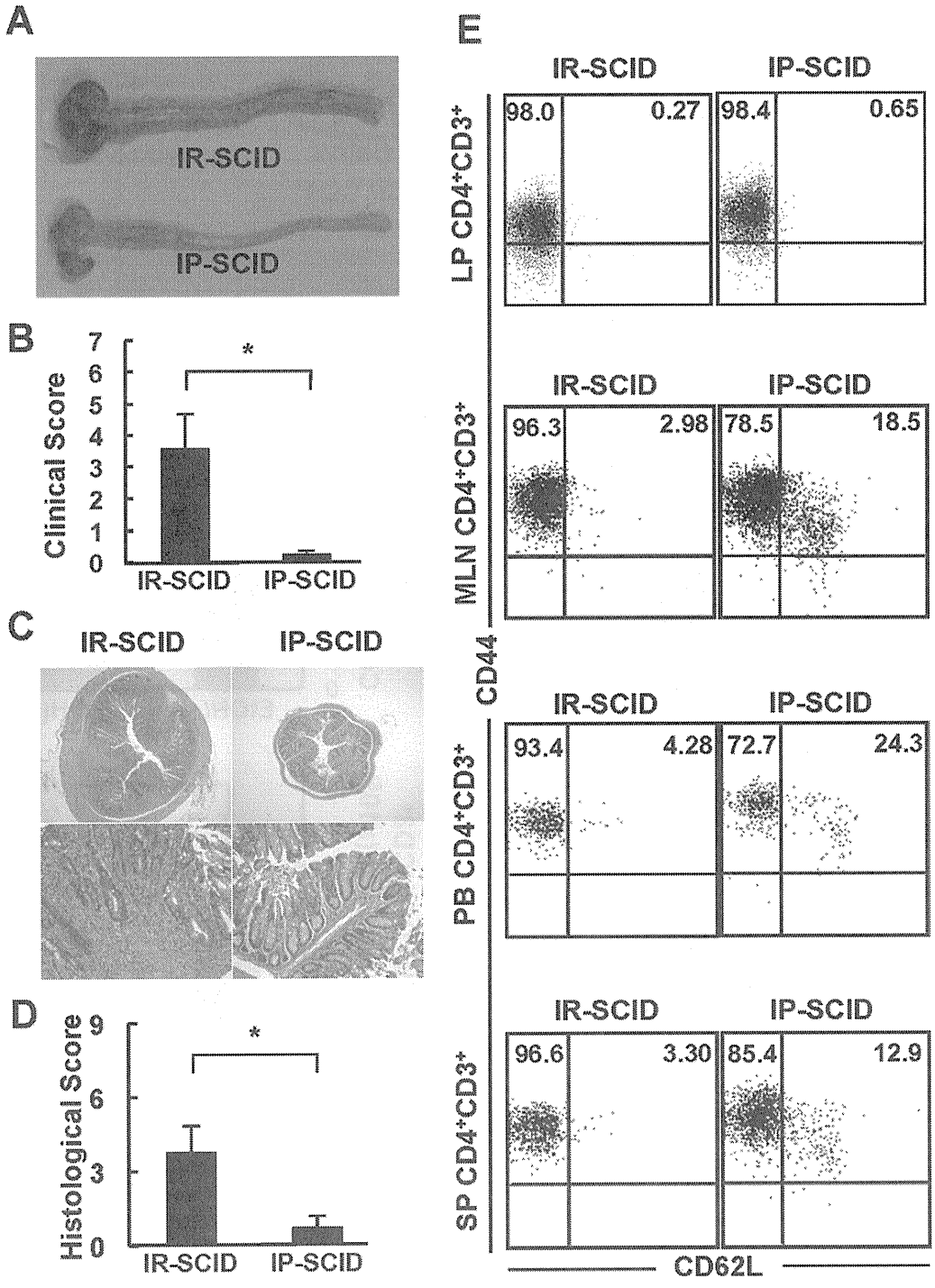

Supplementary Figure 2. Intrarectal administration of splenic CD4+ T cells into SCID mice induces chronic colitis. C.B-17 SCID recipient mice were administered with splenic CD4+ T cells from normal BALB/c mice intrarectally (5×10^6, IR-SCID mice, n = 9) or intraperitoneally (5×10^5, IP-SCID mice, n = 9). (*A*) Gross appearance of the colon from IR- and IP-SCID mice at 10 weeks after cell administration. (*B*) Clinical scores were determined at 10 weeks after administration as described in the Materials and Methods section. Data are indicated as the mean ± standard error of mean (SEM) of 9 mice in each group. *$P < .01$. (*C*) Histologic examination of the colon at 10 weeks after administration. Original magnification, ×40 (*upper panel*) and ×100 (*lower panel*). (*D*) Histologic scores were determined at 10 weeks after transfer as described in the Materials and Methods section. Data are indicated as mean ± SEM of 9 mice in each group. *$P < .05$. (*E*) Phenotypic characterization of $CD3^+CD4^+$-gated T cells expressing CD44/CD62L in lamina propria (*LP*), mesenteric lymph node (MLN), peripheral blood (*PB*), and spleen (*SP*) of each group. Representatives of 9 separate samples in each group.

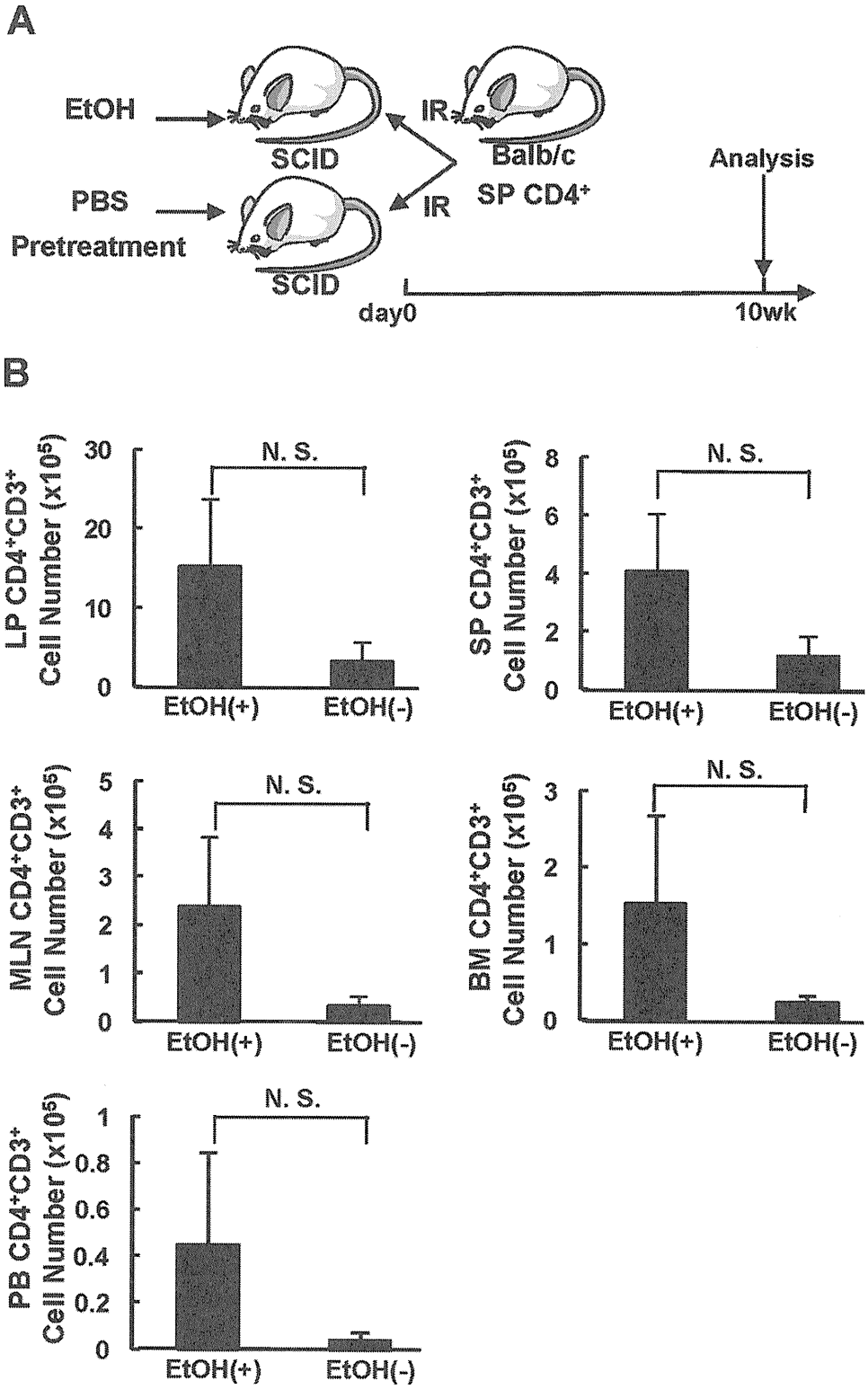

Supplementary Figure 3. Intrarectal administration of splenic $CD4^+$ T cells into SCID mice induces chronic colitis. (*A*) C.B-17 SCID recipient mice with or without pretreatment with 50% ethanol were intrarectally administered 5×10^6 $CD4^+$ T cells from normal BALB/c mice (n = 5 in each group). (*B*) LP, MLN, and spleen $CD3^+CD4^+$ T cells were isolated from the colon at 10 weeks after T-cell administration, and the number of $CD3^+CD4^+$ cells was determined by flow cytometry. Data are indicated as the mean ± standard error of mean of 9 mice in each group. *N. S.*, not significant.

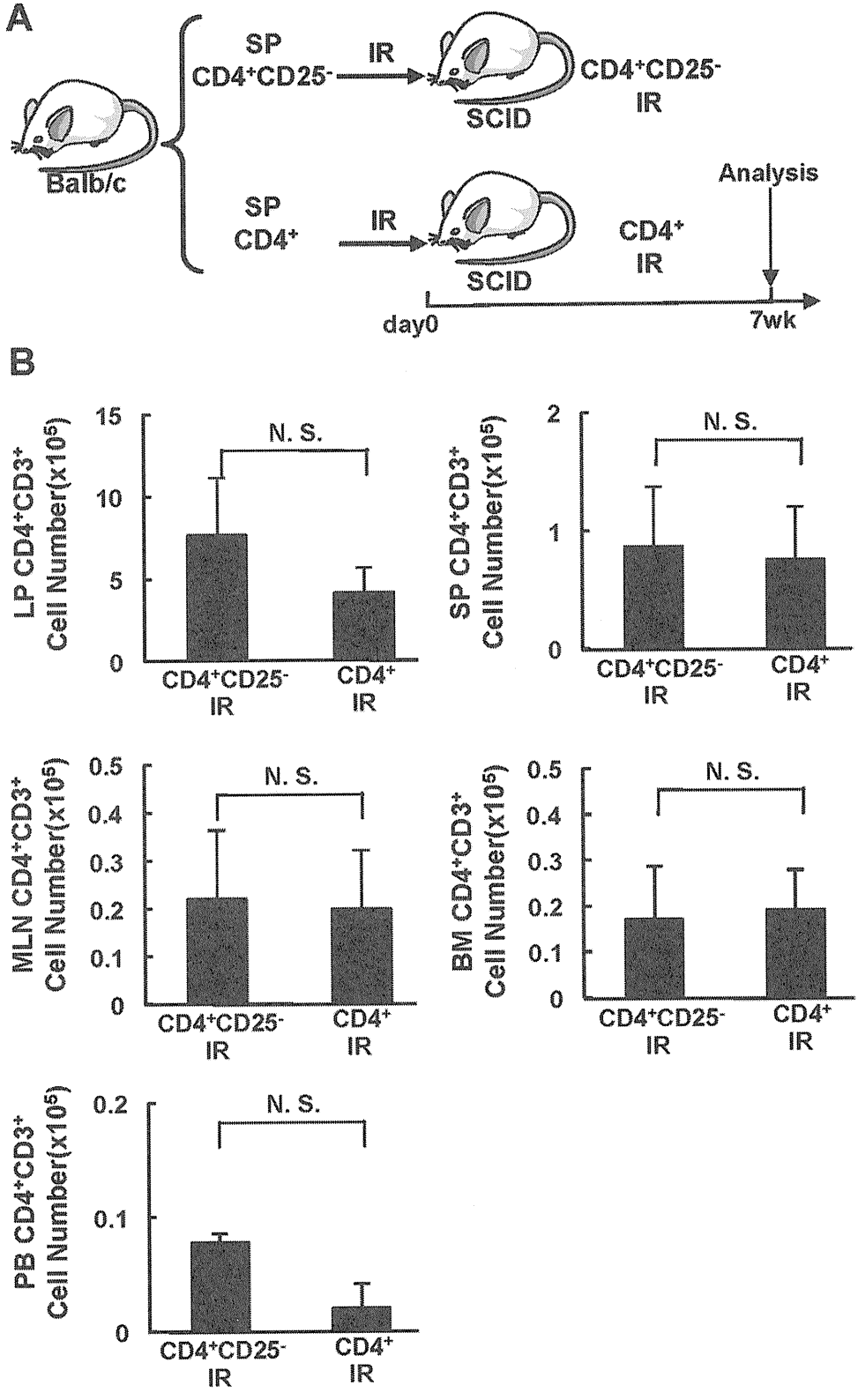

Supplementary Figure 4. SCID mice intrarectally administered with whole $CD4^+$ or $CD4^+CD25^-$ T cells similarly develop colitis. (*A*) C.B-17 SCID recipient mice were intrarectally administered 5×10^6 whole $CD4^+$ T cells or $CD4^+CD25^-$ T cells from normal BALB/c mice. (n = 5 in each group) (*B*) LP, MLN, and spleen $CD3^+CD4^+$ T cells were isolated from the colon at 7 weeks after T-cell administration, and the number of $CD3^+CD4^+$ cells was determined by flow cytometry. Data are indicated as the mean ± SEM of nine mice in each group. *N. S.*, not significant.

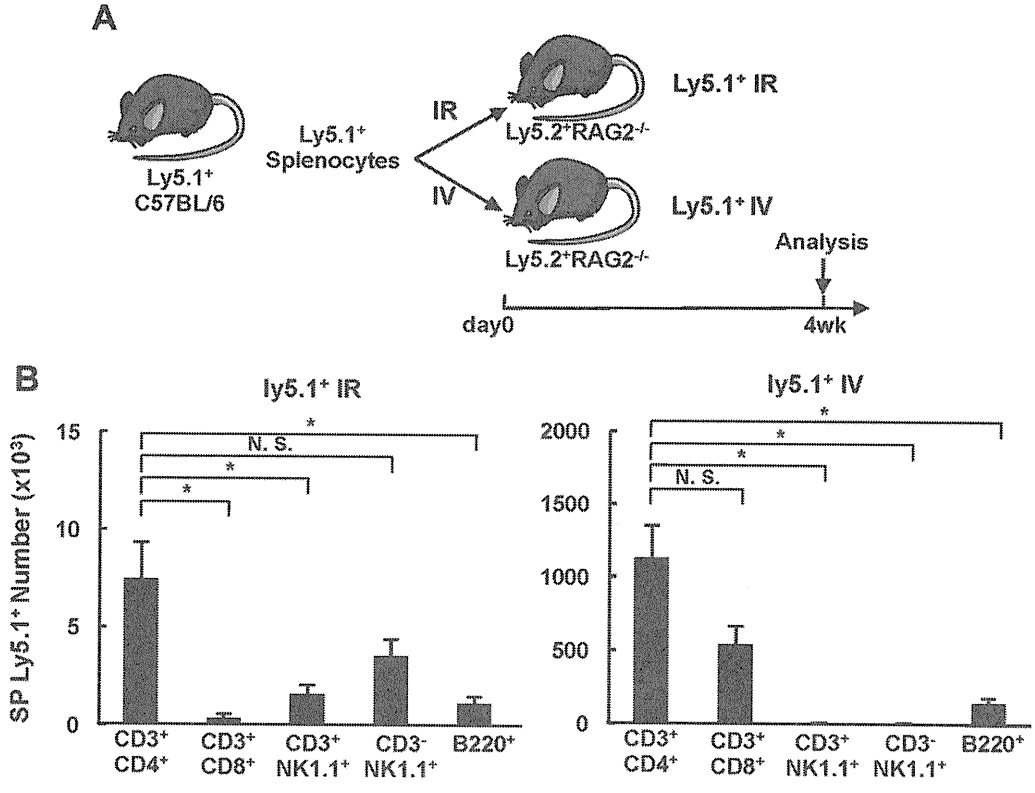

Supplementary Figure 5. Various Ly5.1$^+$ lymphocytes can be detected in SP of RAG-2$^{-/-}$ mice intrarectally administered with Ly5.1$^+$ splenocytes. (*A*) One $\times$ 10^8 splenocytes from Ly5.1$^+$ C57BL/6 mice were intrarectally administered to Ly5.2$^+$RAG-2 recipients (Ly5.1$^+$ IR). As a positive control, 1 $\times$ 10^7 splenocytes from Ly5.1$^+$ C57BL/6 mice were intravenously administered to Ly5.2$^+$RAG-2 recipients (Ly5.1$^+$ IR) (n = 5 in each group). (*B*) Splenocytes were isolated from mice in each group at 4 weeks after T-cell administration, and the number of Ly5.1$^+$CD3$^+$CD4$^+$ (CD4$^+$ T), Ly5.1$^+$CD3$^+$CD8$^+$ (CD8$^+$ T), Ly5.1$^+$CD3$^+$NK1.1$^+$ (NKT), Ly5.1$^+$CD3$^-$NK1.1$^+$ (NK), B220$^+$ (B) cells were determined by flow cytometry. Data are indicated as the mean $\pm$ standard error of mean of 9 mice in each group. *$P < .01$. *N. S.*, not significant.

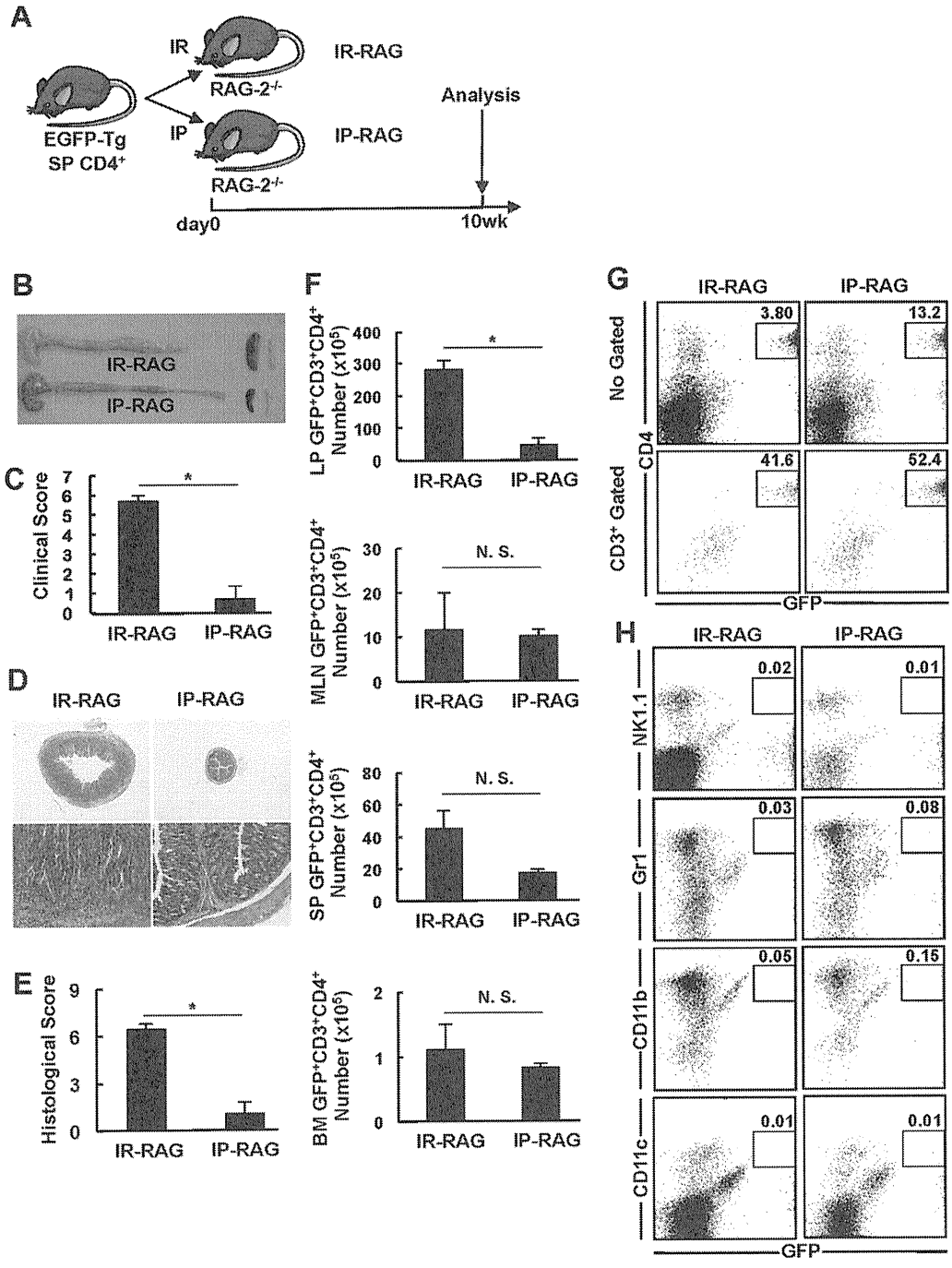

Supplementary Figure 6. Intrarectal administration of splenic GFP$^+$CD4$^+$ T cells into RAG-2$^{-/-}$ mice induces chronic colitis. (*A*) RAG-2$^{-/-}$ mice were administered with CD4$^+$ T cells from CAG-GFP transgenic mice intrarectally (5 × 10^6, IR-RAG, mice, n = 3) or intraperitoneally (5 × 10^5, IP-RAG mice, n = 3). (*B*) Gross appearance of the colon from IR- and IP-RAG mice at 10 weeks after cell administration. (*C*) Clinical scores were determined at 10 weeks after administration as described in Supplementary Materials and Methods section. Data are indicated as the mean ± standard error of mean (SEM) of 3 mice in each group. *P = .0026. (*D*) Histologic examination of the colon at 10 weeks after administration. Original magnification, ×20 (*upper panel*) and ×200 (*lower panel*). (*E*) Histologic scores were determined at 10 weeks after transfer as described in Supplementary Materials and Methods section. Data are indicated as mean ± SEM of 3 mice in each group. *P = .0018. (*F*) Lamina propria (*LP*), mesenteric lymph node (*MLN*), spleen (*SP*), and bone marrow (*BM*) cells were isolated from the colon at 10 weeks after T-cell administration, and the absolute number of GFP$^+$CD3$^+$CD4$^+$ cells was determined by FACS. Data are indicated as the mean ± SEM of 9 mice in each group. *P = .0015. N. S. means not significant difference. (*G*) Expression of GFP in whole CD4$^+$ cells (*upper panel*) and CD3-gated CD4$^+$ cells (*lower panel*) on GFP$^+$ cells of SP from RAG-2$^{-/-}$ mice in each group were assessed by FACS. *Dot plot* is representative one of each group. Representatives of 9 separate samples in each group. (*H*) Endogenous cell surface markers on cells of spleen from each group were assessed by FACS. *Dot plot* analysis of FACS is representative one of each group. Representatives of 3 separate samples in each group.

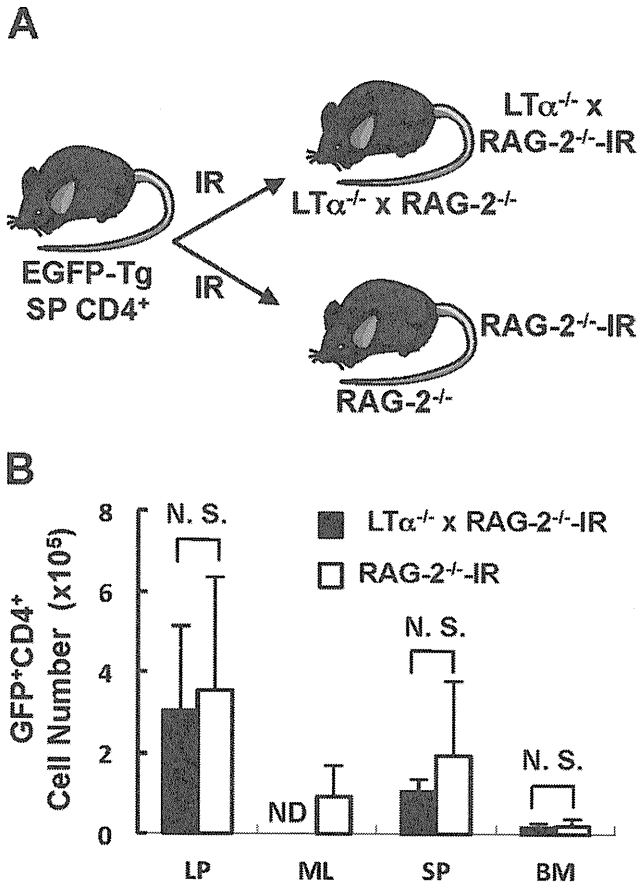

Supplementary Figure 7. Egress of $CD4^+$ T cells from LP is independent of Gut-associated lymphoid tissue (GALT). (*A*) Lymphotoxin α-deficient ($LT\alpha^{-/-}$) × $RAG\text{-}2^{-/-}$ mice or $RAG\text{-}2^{-/-}$ mice were administered $CD4^+$ T cells from CAG-GFP Tg mice intrarectally (1×10^7) and were killed at 14 days after administration. (*B*) Cells were isolated from LP, MLN, SP and BM at 14 days after administration, and the number of GFP^+CD4^+ T cells was determined by flow cytometory. Data are indicated as the mean ± standard error of mean of 5 mice in each group. *$P < .05$. *N. S.*, not significant.

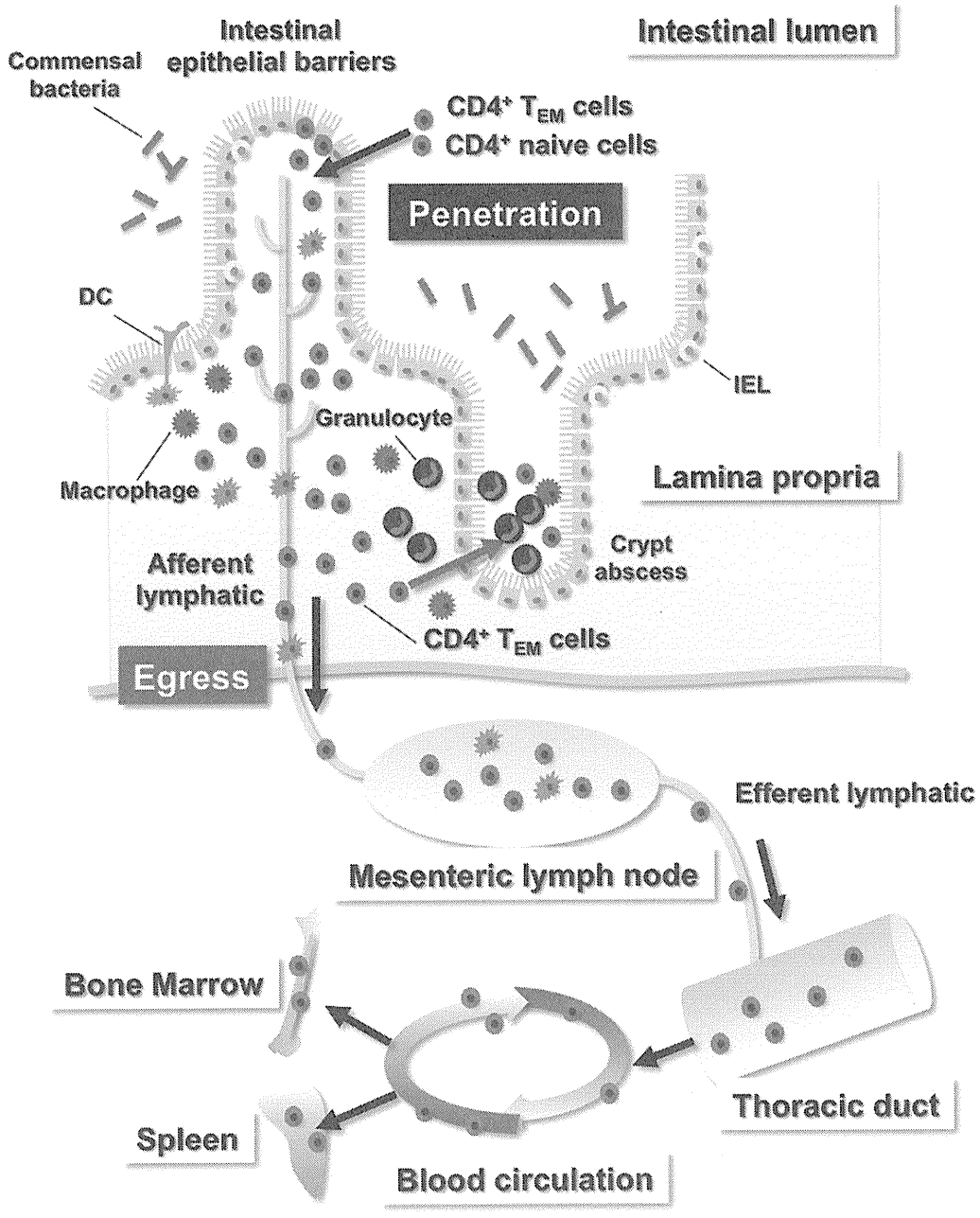

Supplementary Figure 8. Model of CD4+ T-cell penetration across intestinal barriers and its egress from LP to systemic circulation. CD4+ T cells not only penetrate from the intestinal luminal side to the LP but also egress from the LP to the bloodstream in a CCR7-independent manner.

Supplementary Table 2. Antibodies Used in the Study

Antibodies	Manufactures	Antigen retrieval method	Buffer pH for the retrieval	Working dilution	Incubation time and temperature	Second antibody
CD20	Dako, Glostrup, Denmark	MW, 40 min	9.0	1:1	1 h, RT	ABC
CD3	Novocastra, Newcastle, UK	MW, 40 min	9.0	1:20	1 h, RT	ABC
CD4	Novovastra, Newcastle, UK	AC, 20 min	9.0	1:50	24 h, 4°C	ABC
CD8	Dako, Glostrup, Denmark	AC, 20 min	6.0	1:100	24 h, 4°C	ABC
CD56	Novovastra, Newcastle, UK	AC, 20 min	6.0	1:500	24 h, 4°C	ABC
MPO	Dako, Glostrup, Denmark	MW, 40 min	9.0	1:4000	1 h, RT	EnVision

ABC, ABC immunoperoxidase kit (Vector Laboratories, Burlingame, CA); AC, autoclave; EnVision, EnVision+ System (Dako); RT, room temperature; MPO, myeloperoxidase; MW, microwave.

HLA-Cw*1202-B*5201-DRB1*1502 Haplotype Increases Risk for Ulcerative Colitis but Reduces Risk for Crohn's Disease

YUKINORI OKADA,[*,‡] KEIKO YAMAZAKI,[§] JUNJI UMENO,[§,#] ATSUSHI TAKAHASHI,[*] NATSUHIKO KUMASAKA,[*] KYOTA ASHIKAWA,[§] TOMOMI AOI,[§] MASAKAZU TAKAZOE,[‖] TOSHIYUKI MATSUI,[¶] ATSUSHI HIRANO,[#] TAKAYUKI MATSUMOTO,[#] NAOYUKI KAMATANI,[*] YUSUKE NAKAMURA,[**] KAZUHIKO YAMAMOTO,[‡,‡‡] and MICHIAKI KUBO[§]

Laboratory for Statistical Analysis, Center for Genomic Medicine, RIKEN, Yokohama Institute; [‡]Department of Allergy and Rheumatology, Graduate School of Medicine, University of Tokyo, Tokyo; [§]Laboratory for Genotyping Development, Center for Genomic Medicine, RIKEN, Yokohama Institute; [‖]Department of Medicine, Division of Gastroenterology, Social Insurance Chuo General Hospital, Tokyo; [¶]Department of Gastroenterology, Fukuoka University, Chikushi Hospital, Fukuoka; [#]Department of Medicine and Clinical Science, Graduate School of Medical Sciences, Kyushu University, Fukuoka; [**]Laboratory of Molecular Medicine, Human Genome Center, Institute of Medical Science, University of Tokyo, Tokyo; [‡‡]Laboratory for Autoimmune Diseases, Center for Genomic Medicine, RIKEN, Yokohama Institute, Japan

BACKGROUND & AIMS: There are many genetic factors that are associated with both ulcerative colitis (UC) and Crohn's disease (CD). However, genetic factors that have distinct effects on UC and CD have not been examined. **METHODS:** We performed a comparative genome-wide association study (GWAS) and a replication study using data from 748 patients with UC and 979 with CD, selected from a Japanese population. We conducted high-resolution (4-digit) genotyping of human leukocyte antigen (HLA) alleles in patients with UC and CD and additional 905 healthy individuals (controls). We performed haplotype-based analysis using data from the GWAS and HLA alleles to associate them with UC or CD. **RESULTS:** The comparative GWAS and the replication study identified significant associations in the major histocompatibility complex region at 6p21 with UC and CD (rs9271366, $P = 1.6 \times 10^{-70}$; odds ratio [OR] = 4.44). Haplotype-based analysis in the major histocompatibility complex region showed that HLA-Cw*1202-B*5201-DRB1*1502 haplotype was significantly associated with increased risk of UC compared with CD ($P = 1.1 \times 10^{-33}$; OR = 6.58), accounting for most of the associations observed in the GWAS. Compared with the controls, this HLA haplotype significantly increases susceptibility to UC ($P = 4.0 \times 10^{-21}$; OR = 2.65), but reduces risk for CD ($P = 1.1 \times 10^{-7}$; OR = 0.40). Distinct effects of this HLA haplotype on UC and CD were independent of other HLA alleles and haplotypes ($P = 2.0 \times 10^{-19}$ and $P = 7.2 \times 10^{-5}$, respectively). **CONCLUSIONS: The HLA-Cw*1202-B*5201-DRB1*1502 haplotype increases susceptibility to UC but reduces risk for CD, based on a GWAS of a Japanese population.**

Keywords: Inflammatory Bowel Disease; Genetics; Risk Factor; Susceptibility.

Ulcerative colitis (UC) and Crohn's disease (CD), the 2 main subtypes of inflammatory bowel disease (IBD), are chronic relapsing inflammatory disorders of the digestive tract. Although aberrant responses of the intestinal immune system in genetically predisposed individuals play an important role in the pathogenesis of both diseases, typical features of UC and CD differ with respect to disease localization and histological findings.[1,2] CD most commonly involves the ileum and colon, but can affect any region of the gut, whereas UC always involves the rectum and extends as far as the cecum. Pathologically, inflammatory change is transmural and often discontinuous in CD, but it typically involves only superficial mucosal and submucosal layers of the intestinal wall with a continuous pattern in UC. Moreover, Th1- and Th17-associated cytokines are markedly increased in the inflamed mucosa of CD, whereas Th2-associated cytokines seem to be increased in that of UC.[3] These findings suggest that some genetic or environmental factors that differentiate UC and CD might exist.

A number of genome-wide association studies (GWAS) have identified numerous susceptibility loci for UC and CD.[4–17] Among them, *NKX2-3* and multiple genes involved in the interleukin-23 signaling pathway have been reported to be associated with both UC and CD.[16,18–20] In contrast, alterations in genes of innate immune system and autophagy are considered to be specific to CD.[14,18,19] However, current evidence is insufficient to explain the differences in the clinical manifestations between UC and CD. Previous studies have shown that the same alleles in particular genes sometimes have opposite directions of effects on different autoimmune disorders.[15,21] Therefore, finding additional variants with distinct effects on UC and CD will provide important clues for further understanding of the pathogenesis of both diseases.

To identify the genetic factors that have distinct role between UC and CD, we performed a comparative GWAS that directly compared UC and CD cases in the Japanese

Abbreviations used in this paper: CD, Crohn's disease; CI, confidence interval; DC, dendritic cell; GWAS, genome-wide association study; HLA, human leukocyte antigen; IBD, inflammatory bowel disease; LD, linkage disequilibrium; MHC, major histocompatibility complex; OR, odds ratio; SNP, single nucleotide polymorphisms; UC, ulcerative colitis.

0016-5085/$36.00
doi:10.1053/j.gastro.2011.05.048

Table 1. Basic Characteristics of Study Subjects

Set	CD cases		UC cases		
	GWAS	Replication	GWAS	Replication	Control
No. of samples	372	607	372	376	905
Male, n (%)	266 (71.5)	416 (68.5)	172 (46.2)	188 (50.0)	671 (74.1)
Age at sampling (*y*), mean ± SD	33.9 ± 9.4	39.1 ± 12.7	42.6 ± 16.1	43.8 ± 15.6	52.5 ± 14.4
Characteristics of CD					
Age at disease onset, n (%)					
≤16 (A1)	61 (16.5)	68 (11.2)			
17–40 (A2)	296 (80.2)	465 (76.6)			
>40 (A3)	12 (3.3)	74 (12.2)			
Disease location, n (%)					
Ileal disease (L1)	153 (41.6)	235 (38.8)			
Colonic disease (L2)	54 (14.7)	98 (16.2)			
Ileocolonic disease (L3)	158 (42.9)	272 (44.9)			
Upper gastrointestinal disease (L4)	3 (0.8)	1 (0.2)			
Disease behavior, n (%)					
Nonstricturing, nonpenetrating (B1)	101 (27.5)	171 (28.2)			
Stricturing (B2)	185 (50.4)	229 (37.7)			
Penetrating (B3)	81 (22.1)	207 (34.1)			
Perianal disease modifier	150 (40.9)	316 (52.1)			
Characteristics of UC					
Disease extent, n (%)					
Ulcerative proctitis (E1)			51 (14.0)	68 (18.4)	
Left-sided UC (E2)			141 (38.7)	133 (36.0)	
Extensive UC (E3)			172 (47.3)	168 (45.5)	

SD, standard deviation.

population. This approach effectively enabled the identification of the genetic factor with distinct effects. Because previous studies reported that the several HLA alleles were associated with UC or CD,[22–25] we genotyped high-resolution HLA alleles of the subjects. Through an intensive analysis integrating the GWAS data and HLA allele genotypes, our study provided evidence that a particular HLA haplotype independently confers opposite directions of genetic effects on UC and CD.

Materials and Methods

Subjects

A total of 752 individuals with UC and 983 individuals with CD, all of Japanese descent, were enrolled in the study. Subjects with UC were collected from the Kyushu University and 25 affiliated hospitals as described previously[15] and randomly divided into the GWAS set (n = 376) and replication set (n = 376). Subjects with CD were collected at the Social Insurance Chuo General Hospital (n = 376 for GWAS set, overlapping with the cases of the previous study[4]) and the Kyushu University with 16 affiliated hospitals (n = 607 for replication set). The diagnosis of UC or CD in all subjects was made by expert gastroenterologists in accordance with clinical, radiological, endoscopic, and histological features according to the Lennard-Jones' criteria.[26] Patients with indeterminate colitis were excluded in advance. After applying quality control measures (see the next section), we analyzed a total of 748 UC cases and 979 CD cases (Table 1). For the control subjects, we used healthy volunteers recruited at the Midosuji and other related Rotary Clubs (n = 905). These subjects had been included in our previous studies.[4,15,27] The subjects who were determined to be of non-Japanese origin, by self-report or by principal component analysis, were excluded. All individuals enrolled in the study gave their written informed consent, and approval was obtained from the ethical committees at Kyushu University, Social Insurance Chuo General Hospital, and RIKEN Yokohama Institute.

Genotyping and Quality Control in the Comparative GWAS

In the comparative GWAS, 376 UC cases and 376 CD cases were genotyped with >550,000 single nucleotide polymorphisms (SNPs) using Illumina HumanHap550v3 Genotyping BeadChip (Illumina, San Diego, CA). After excluding subjects with call rates <0.98, SNPs with call rates <0.99 in UC cases or CD cases or nonautosomal SNPs were excluded. We excluded closely related subjects using identity-by-descent estimated by PLINK version 1.06.[28] For pairs in a first or second degree of kinship, we excluded the subjects who had lower call rate than the other. To evaluate potential population stratification in our study population, we performed principal component analysis for the GWAS data along with European, African, and East-Asian (Japanese and Han Chinese) individuals obtained from Phase II HapMap database (release 22)[29] using EIGENSTRAT version 2.0.[30] We excluded SNPs with minor allele frequency <0.01 in UC cases or CD cases.

Genotyping and Quality Control in the Replication Study

To validate the associations observed in our comparative GWAS, we performed a replication study using independent individuals of 376 UC and 607 CD. We selected the most significantly associated SNPs for each of the loci that showed $P < 1.0 \times 10^{-4}$ in the GWAS. Genotyping of the SNPs was performed for UC and CD cases using multiplex polymerase chain reaction–based Invader assay. To evaluate how the signif-

icant associations between UC and CD reflected the risk of UC and CD, we additionally genotyped the SNPs with those of 905 healthy controls. Genotyping for the healthy controls were performed using Illumina HumanHap550v3 Genotyping BeadChip, and the same quality control criteria in the GWAS were applied.

Genotyping of HLA Alleles

To comprehensively evaluate the associations with UC and CD in the major histocompatibility complex (MHC) region, we performed a high-resolution (4-digit) genotyping of HLA-C, HLA-B, HLA-DRB1, and HLA-DPB1 alleles for UC and CD cases enrolled in the GWAS and the healthy controls. Genotyping of the HLA alleles was performed using WAKFlow HLA typing kit (Wakunaga, Hiroshima, Japan) and a Luminex Multi-Analyte Profiling system (xMAP; Luminex, Austin, TX), according to manufacturer's instructions.

Statistical Analysis

The association of the SNP in the GWAS and the replication study was tested with the Cochran-Armitage trend test. Combined analysis was performed with the Mantel-Haenszel method. Comparison of HLA allele frequency was assessed by the χ^2 test for an allelic 2 × 2 contingency table, and odds ratio (OR) and 95% confidence interval (CI) were estimated using Woolf's method. Fisher's exact test was performed for the tables with expected cell values <5. Bonferroni correction based on the number of the observed alleles were applied for the analysis of HLA alleles and haplotypes (α = .05). Linkage disequilibrium (LD) index, r^2, among HLA alleles were calculated using Haploview version 4.0.[31] LD structure of HLA alleles were visualized using textile plot, a graphical representation for high-dimensional multivariable data, which may help to understand underlying LD patterns hard to capture by conventional triangular heat map display of LD index.[32] Haplotype frequency was estimated by the expectation-maximization algorithm using the haplo.stats package version 1.4.4.[33] No cutoff threshold of haplotype frequency was assigned in the estimation. Association analysis of the haplotype was performed using haplo.glm function implemented in haplo.stats.[33] The haplotype with the highest frequency was adopted as the base haplotype. In multivariate regression analysis, HLA haplotypes and alleles significantly associated between UC and CD were adopted as independent variables. Associations were assessed using logistic regression model assuming additive effects of the expected dosages of the HLA haplotypes and the genotype counts of the HLA alleles. Proportion of the risk explained by HLA haplotypes and alleles was estimated using population attributable risk[34] based on ORs obtained in the multivariate logistic regression model. Independent association of the SNP was tested with multivariate logistic regression model assuming additive effect with adjustment for the HLA haplotypes and alleles as independent covariates. *R* software version 2.9.0 (http://cran.r-project.org) was used for general statistical analysis.

Results

Comparative GWAS Between UC and CD

In the comparative GWAS, 3 UC cases and 2 CD cases were excluded due to low call rates, and 1 UC case and 2 CD cases were excluded due to close relationships. A principal component analysis plot clearly separated the subjects into 3 clusters as indicated previously (Supplementary Figure 1).[35] Our study population was in concordance with the cluster of East-Asian individuals and no outlier was detected, suggesting homogeneous ancestries of our study population. Finally, 461,368 autosomal SNPs for 372 UC cases and 372 CD cases fulfilled the quality-control criteria.

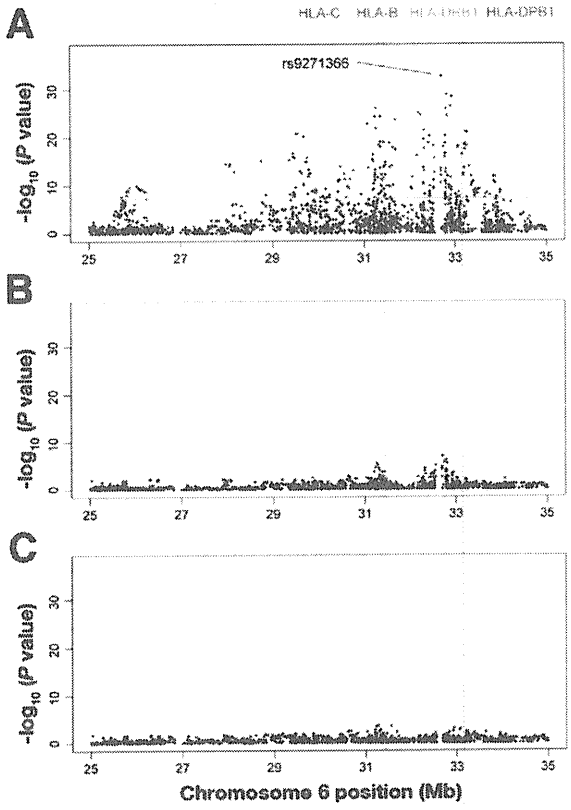

Figure 1. Result of the comparative GWAS using 372 UC cases and 372 CD cases around the MHC region (Chr. 6, 25–35 Mb). Positional plots of $-\log_{10}$ (*P* value) of the SNPs (*A*) before adjustment, (*B*) after adjustment of HLA-Cw*1202-B*5201-DRB1*1502 haplotype, and (*C*) after adjustment of the all associated HLA haplotypes and alleles including HLA-Cw*1202-B*5201-DRB1*1502, HLA-Cw*1402-B*5101, DRB1*0405, DRB1*1501, and DPB1*0501. The *gray horizontal lines* in the plots represent the genome-wide significance threshold of $P = 5.0 \times 10^{-8}$.

We evaluated the associations of the SNPs between UC and CD, and identified significant associations that satisfied the genome-wide significance threshold of $P < 5.0 \times 10^{-8}$ in the MHC region (Figure 1*A*, Supplementary Figure 2). After excluding the SNPs in the MHC region, no remarkable discrepancy from null hypothesis was suggested with the inflation factor, λ_{GC}, being 1.09 (Supplementary Figure 3).

Replication Study

To find additional genetic loci that have distinct role between UC and CD, we selected candidate SNPs that showed $P < 1.0 \times 10^{-4}$ for the replication study. We evaluated the associations for 52 loci and found signifi-

cant associations for rs9271366 and rs2006996 after Bonferroni correction ($P < .05/52$). The combined analysis of the GWAS and the replication study revealed that 2 loci reached genome-wide significance level ($P < 5.0 \times 10^{-8}$) of associations (rs9271366 located close to *HLA-DRB1* at 6p21, $P = 1.6 \times 10^{-70}$, OR = 4.44, 95% CI: 3.74−5.27; rs2006996 in the *TNFSF15* locus at 9q32, $P = 3.7 \times 10^{-13}$, OR = 0.60, 95% CI: 0.52−0.69; Table 2). Statistical power of this study was estimated to be 54.7% under the assumption of the risk variant with OR of 1.5 and allele frequency of 0.3 ($\alpha = 5.0 \times 10^{-8}$).

When the frequencies of the 2 SNPs in UC or CD cases were compared with those of 905 healthy controls, the C allele of rs2006996 in the *TNFSF15* locus showed a significant susceptible effect on CD ($P = 3.7 \times 10^{-16}$, OR = 1.75, 95% CI: 1.53−1.99), but did not show any association with UC ($P = 0.54$, OR = 1.04, 95% CI: 0.91−1.20), which was compatible with the previous report.[4] On the other hand, the C allele of rs9271366 in the MHC region demonstrated a significant susceptible effect on UC ($P = 3.4 \times 10^{-31}$, OR = 2.41, 95% CI: 2.07−2.81), but showed a protective effect on CD ($P = 8.3 \times 10^{-11}$, OR = 0.56, 95% CI: 0.47−0.67; Table 2).

Associations of HLA Alleles

A total of 22 HLA-C alleles, 39 HLA-B alleles, 32 HLA-DRB1 alleles, and 17 HLA-DPB1 alleles were genotyped. In the comparison of the HLA allele frequencies between UC and CD cases, significant associations were observed in 2 HLA-C alleles, 2 HLA-B alleles, 3 HLA-DRB1 alleles, and 2 HLA-DPB1 alleles after Bonferroni correction ($\alpha = .05$, n = 110, $P < .00045$; Table 3 and Supplementary Table 1). Several HLA alleles, namely Cw*1202, B*5201, DRB1*1502, and DPB1*0901, conferred strong associations between UC and CD ($P < 1.0 \times 10^{-23}$). These HLA alleles also showed susceptible effects on UC ($P < 1.0 \times 10^{-12}$, OR ranged from 2.25 to 2.62), but showed protective effects on CD ($P < 5.0 \times 10^{-5}$, OR ranged from 0.40 to 0.52). On the other hand, DRB1*0405 indicated significant association between UC and CD ($P = 2.4 \times 10^{-8}$), with susceptible effect on CD ($P = 3.8 \times 10^{-7}$) and no significant association with UC ($P = .072$). These results were compatible with the previously reported associations of B*5201 and DRB1*1502 with UC,[22–24] or DR4 alleles with CD.[23,24]

LD Structure of HLA Alleles

Because strong and complex LD pattern exists throughout the MHC region,[36,37] we evaluated the LD among the HLA alleles associated between UC and CD. A triangular heat map display of LD index in the controls demonstrated that strong LD existed among Cw*1202, B*5201, and DRB1*1502, and between Cw*1402 and B*5101 ($r^2 > 0.75$) (Figure 2*A*). Visualization of LD structure of these HLA alleles using textile plot clearly showed that Cw*1202, B*5201, and DRB1*1502 composed one long-range haplotype (Figure 2*B*). Moreover, this haplotype was distinctly isolated from other HLA alleles in its vertical po-

Table 2. Significantly Associated SNPs Between UC Cases and CD Cases

rsID	Chr	Position	Gene	Allele 1/2	Study Set	No. of subjects UC	CD	Control	Allele 1 frequency UC	CD	Control	UC vs CD OR (95% CI)	UC vs CD *P* value[a]	UC vs control OR (95% CI)	UC vs control *P* value[a]	CD vs control OR (95% CI)	CD vs control *P* value[a]
rs9271366	6	32,694,832	MHC Region	C/T	GWAS	372	372	—	0.37	0.10	—	5.21 (3.94–6.90)	6.1×10^{-34}	—		—	
					Replication	376	607	—	0.40	0.14	—	3.97 (3.20–4.94)	4.5×10^{-36}	—		—	
					Combined	748	979	905	0.39	0.13	0.21	4.44 (3.74–5.27)	1.6×10^{-70}	2.41 (2.07–2.81)	3.4×10^{-31}	0.56 (0.47–0.67)	8.3×10^{-11}
rs2006996	9	116,632,459	*TNFSF15*	C/T	GWAS	372	372	—	0.55	0.65	—	0.65 (0.53–0.80)	6.2×10^{-5}	—		—	
					Replication	376	607	—	0.53	0.67	—	0.56 (0.46–0.67)	1.0×10^{-9}	—		—	
					Combined	748	979	905	0.54	0.66	0.53	0.60 (0.52–0.69)	3.7×10^{-13}	1.04 (0.91–1.20)	0.54	1.75 (1.53–1.99)	3.7×10^{-16}

[a]Obtained by Cochran–Armitage trend test for the GWAS and the replication study, by Mantel–Haenzel test for the combined study.

Table 3. Significantly Associated HLA-C/B/DRB1/DPB1 Alleles Between UC Cases and CD Cases

	Allele frequency			UC vs CD		UC vs control		CD vs control	
HLA allele	UC (n = 372)	CD (n = 372)	Control (n = 905)	OR (95% CI)	*P* value	OR (95% CI)	*P* value	OR (95% CI)	*P* value
HLA-C									
Cw*1202	0.29	0.077	0.14	4.98 (3.64–6.81)	7.4×10^{-27}	2.57 (2.09–3.17)	5.5×10^{-20}	0.52 (0.38–0.70)	1.3×10^{-5}
Cw*1402	0.050	0.11	0.074	0.42 (0.28–0.62)	1.1×10^{-5}	0.65 (0.45–0.95)	.026	1.58 (1.18–2.10)	.0019
HLA-B									
B*5101	0.063	0.13	0.088	0.46 (0.32–0.66)	2.3×10^{-5}	0.69 (0.50–0.97)	.033	1.51 (1.15–1.97)	.0028
B*5201	0.29	0.075	0.14	5.09 (3.72–6.98)	2.3×10^{-27}	2.62 (2.13–3.22)	1.6×10^{-20}	0.51 (0.38–0.70)	1.3×10^{-5}
HLA-DRB1									
DRB1*0405	0.10	0.21	0.13	0.44 (0.33–0.59)	2.4×10^{-8}	0.78 (0.59–1.02)	.072	1.78 (1.42–2.23)	3.8×10^{-7}
DRB1*1501	0.093	0.043	0.070	2.26 (1.46–3.48)	.00016	1.37 (1.01–1.86)	.044	0.61 (0.41–0.90)	.013
DRB1*1502	0.28	0.060	0.14	6.09 (4.31–8.59)	3.2×10^{-29}	2.46 (1.99–3.03)	9.8×10^{-18}	0.40 (0.29–0.56)	4.0×10^{-8}
HLA-DPB1									
DPB1*0501	0.38	0.46	0.39	0.69 (0.56–0.85)	.00044	0.95 (0.80–1.14)	.60	1.38 (1.16–1.64)	.00023
DPB1*0901	0.24	0.057	0.13	5.36 (3.76–7.63)	7.1×10^{-24}	2.25 (1.81–2.80)	1.2×10^{-13}	0.42 (0.30–0.59)	3.1×10^{-7}

NOTE. HLA alleles that satisfied Bonferroni correction based on the number of the observed alleles in the comparisons of UC and CD cases are indicated ($\alpha = .05$, n = 110, $P < .00045$). Results of all the observed HLA alleles are indicated in Supplementary Table 1.
n, number of subjects enrolled in the analysis.

sition, reflecting strong LD within these alleles and weak LD with other alleles. Interestingly, its frequency was high in UC, middle in controls, and low in CD, suggesting its opposite directions of effects on UC and CD.

Haplotype-Based Analysis of HLA Alleles

We then performed haplotype-based association analysis in strong LD (Table 4). HLA-Cw*1202-B*5201-DRB1*1502 haplotype demonstrated significant associations between UC and CD ($P = 1.1 \times 10^{-33}$, OR = 6.58, 95% CI: 4.60–9.42), with a susceptible effect on UC ($P = 4.0 \times 10^{-21}$, OR = 2.65, 95% CI: 2.14–3.29) and a protective effect on CD ($P = 1.1 \times 10^{-7}$, OR = 0.40, 95% CI: 0.28–0.57). Although HLA-DPB1*0901 was in moderate LD with Cw*1202, B*5201, and DRB1*1502 ($r^2 = 0.54$–0.66), we did not include it in the risk haplotype because both HLA-Cw*1202-B*5201-DRB1*1502-DPB1*0901 and HLA-Cw*1202-B*5201-DRB1*1502-non DPB1*0901 haplotypes indicated significant associations between UC and CD ($P < 1.0 \times 10^{-5}$; data not shown). HLA-Cw*1402-B*5101 haplotype also indicated significant associations between UC and CD ($P = 1.8 \times 10^{-5}$), but their associations with UC and CD were suggestive ($P < .05$).

To account for the relative effects among the HLA alleles and confirm that the distinct effects of HLA-Cw*1202-B*5201-DRB1*1502 haplotype on UC and CD were not the reflection of other UC- or CD-specific effect alleles, we performed a multivariate regression analysis including all the associated HLA haplotypes and alleles (HLA-Cw*1202-B*5201-DRB1*1502, HLA-Cw*1402-B*5101, DRB1*0405, DRB1*1501, and DPB1*0501). This analysis demonstrated a significant association of HLA-Cw*1202-B*5201-DRB1*1502 haplotype ($P = 3.0 \times 10^{-22}$) with a susceptible effect on UC ($P = 2.0 \times 10^{-19}$) and a protective effect on CD ($P = 7.2 \times 10^{-5}$), confirming the distinct effects of this haplotype on UC and CD were independent of other HLA alleles. Combination of these HLA haplotypes and alleles explained 41% of the difference of the risks between UC and CD. Among them, HLA-Cw*1202-B*5201-DRB1*1502 haplotype accounted for 63% of the explained genetic risk of HLA haplotypes and alleles.

When CD cases were stratified by colonic (n = 53) and noncolonic (n = 315) phenotypes, frequencies of HLA-Cw*1202-B*5201-DRB1*1502 haplotype were significantly different among UC, colonic, and noncolonic CD (0.27, 0.10, and 0.043, respectively; $P < .01$; Supplementary Table 2). Compared with the frequency of healthy controls (0.12), HLA-Cw*1202-B*5201-DRB1*1502 haplotype had a significant susceptible effect on UC ($P = 4.0 \times 10^{-21}$, OR = 2.65) and a significant protective effect on noncolonic CD ($P = 5.2 \times 10^{-9}$, OR = 0.32), but had no effect on colonic CD ($P = .58$, OR = 0.83).

Associations of SNPs in MHC Region After Adjustment of HLA Alleles

Because the previous studies supposed that the associations of the SNPs in the MHC region are the reflection of the associations of the HLA alleles via long-

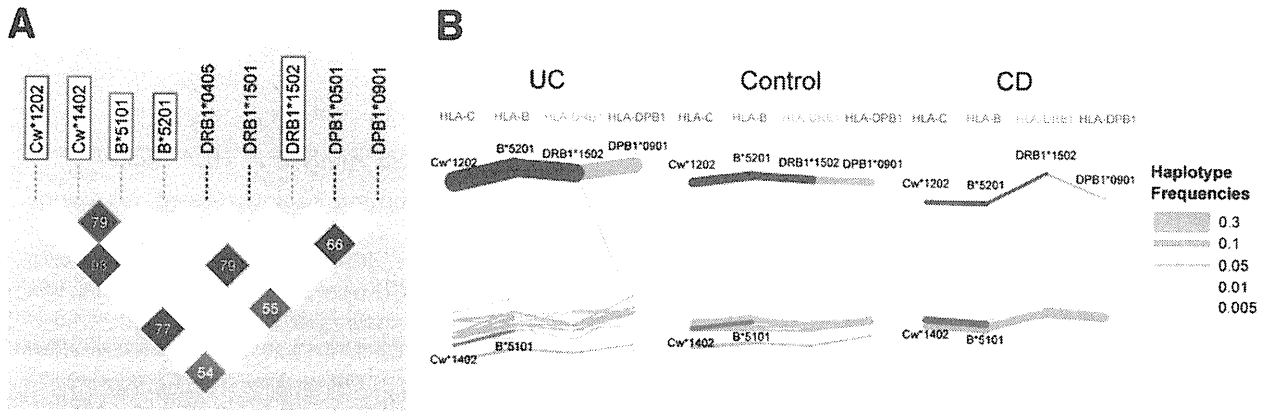

Figure 2. LD map and haplotype structure of HLA alleles. (*A*) Triangular heat map display of LD index, r^2, among the HLA alleles associated between UC and CD. LD map based on the controls is drawn using Haploview version 4.0.[31] r^2 value >0.5 is indicated in the *diamond*. Pairs of the HLA alleles in strong LD ($r^2 > 0.75$) are highlighted with *magenta* or *orange-red*. (*B*) Haplotype structure of HLA alleles represented by textile plot.[32] The *dotted vertical axis* indicates each of the 4 HLA genes, and the queues of the axes correspond to their physical order in the MHC region. A point on an axis indicates an HLA allele, and a segment connects 2 alleles on adjacent genes. The thickness of the segment corresponds to the haplotype frequency between the 2 HLA alleles, relative to thicknesses of lines shown in the legend. The vertical positions of HLA alleles are simultaneously chosen so that all connected segments are aligned as horizontally as possible. Haplotypes consisted of the HLA alleles in strong LD ($r^2 > 0.75$) are highlighted in the same color as in (*A*) along with the names of the alleles. The existence of the haplotype consisting of Cw*1202, B*5201, and DRB1*1502 is clearly shown, although the connection between DRB1*1502 and DPB1*0901 seems relatively weaker. Frequency of the haplotype decays from in order of UC cases, the controls, and CD cases, representing its opposite directions of effects on UC and CD.

range LD with them,[25] we performed the multivariate logistic regression analysis of the SNPs in the MHC region with the adjustment of the identified HLA haplotypes and alleles. After adjusted for HLA-Cw*1202-B*5201-DRB1*1502 haplotype, most of the associations in MHC region were largely weakened (the smallest $P = 1.0 \times 10^{-7}$; Figure 1*B*). When the SNPs were further adjusted for other associated HLA haplotypes and alleles, no significant association was observed (the smallest $P = .00023$; Figure 1*C*). This suggested that HLA-Cw*1202-B*5201-DRB1*1502 accounted for most of the associations in the MHC region observed in our comparative GWAS, and the remaining weak associations could also be attributable to other HLA haplotypes and alleles.

Discussion

Through a comparative GWAS between UC and CD and a follow-up study using high-resolution HLA alleles, we demonstrated that a particular HLA haplotype, HLA-Cw*1202-B*5201-DRB1*1502, independently confers a susceptible effect on UC, but has a protective effect on CD. Although previous studies suggested distinct associations of some HLA-DRB1 alleles with UC and CD,[23,24] their associations were not substantially evaluated.[38] Our study clearly showed that one haplotype extending throughout the MHC class I, III, and II regions confers opposite directions of effects on UC and CD. This haplotype accounted for two thirds of the difference of the genetic risks between UC and CD in the MHC region, suggesting its substantial role in the etiology of IBD. Although recent comparative association studies for IBD mostly identified the risk loci shared between UC and CD,[16,19,21,39] our study is the first to identify the loci with the opposite directions of the effects.

Contrary to our results, the comparative study for IBD in European populations did not demonstrate the distinct effects in the MHC region.[12,16,21] One probable explanation for this discrepancy would be the ethnic differences of haplotype frequencies. According to HapMap populations, frequencies of Cw*1202, B*5201, and DRB1*1502 were relatively high in the Japanese population (0.091 for Cw*1202, 0.091 for B*5201, and 0.102 for DRB1*1502, respectively), but were low in the European population (0.0111 for Cw*1202, 0.0167 for B*5201, and 0.0056 for DRB1*1502, respectively).[36] It would be plausible that the loss of statistical power due to the low haplotype frequency in European populations hampered the detection of the distinct effects on IBD in the MHC region. In addition, our comparative approach by comparing UC and CD directly would have effectively highlighted the distinct effects.

The intestinal immune system is maintained to protect against bacterial infection while avoiding the destructive inflammatory response to normal microbiota. Innate immune cells including dendritic cells (DCs) and macrophages provide the first line of defense against entry of pathogens across the mucosal barrier.[2,40] The entry of pathogenic bacteria activates DCs, and activated DCs present specific MHC class II molecules on its surface. According to this antigen presentation, naïve $CD4^+$ T cells proliferate and differentiate into various effector subsets characterized by the production of distinct cytokines.[41,42] CD have been considered to be a typical Th1 disease that is characterized by overproduction of interferon-γ in the inflamed gut, while UC is referred to as a "Th2-like" or "mixed" phenotype.[3] Several studies showed that immune responses induced by intestinal DCs vary among bacterial pathogens and a distinct differentiation

Table 4. Associations of the Haplotype Consisting of HLA Alleles Associated Between UC Cases and CD Cases

Haplotype			Frequency[a]			UC vs CD		UC vs control		CD vs control	
			UC (n = 372)	CD (n = 372)	Control (n = 905)	OR (95% CI)[b]	P value[b]	OR (95% CI)[b]	P value[b]	OR (95% CI)[b]	P value[b]
Haplotype for Cw*1202, B*5201, DRB1*1502											
Cw*1202	B*5201	DRB1*1502	0.27	0.054	0.12	6.58 (4.60–9.42)	1.1×10^{-33}	2.65 (2.14–3.29)	4.0×10^{-21}	0.40 (0.28–0.57)	1.1×10^{-7}
Cw*1202	B*5201	—	0.025	0.022	0.013	1.51 (0.76–2.97)	.15	2.24 (1.21–4.14)	.0080	1.49 (0.79–2.81)	.21
—	—	DRB1*1502	0.011	0.0056	0.012	2.64 (0.81–8.65)	.030	1.10 (0.49–2.46)	.54	0.42 (0.15–1.19)	.067
—	—	—	0.69	0.92	0.85						
Haplotype for Cw*1402, B*5101											
Cw*1402	B*5101		0.050	0.11	0.072	0.42 (0.28–9.42)	1.8×10^{-5}	0.67 (0.46–0.98)	.039	1.62 (1.21–2.17)	.0010
—	B*5101		0.013	0.016	0.017	0.78 (0.33–1.81)	.57	0.78 (0.38–1.61)	.48	1.01 (0.51–1.98)	.90
—	—		0.94	0.87	0.91						

NOTE. HLA alleles other than Cw*1202, B*5201, DRB1*1502, or Cw*1402, B*5101 are pooled and denoted as "—."
n, Number of subjects enrolled in the analysis.
[a]Haplotype with >0.5% of frequency in the controls are indicated.
[b]Obtained by the comparison of haplotype frequencies between each of the haplotype and the haplotype with the highest frequency.

of Th-cell subsets are induced according to the pathogens.[40,43] These results indicate that the specific pathogens recognized by HLA-Cw*1202-B*5201-DRB1*1502 haplotype will promote the inappropriate proliferation and differentiation of naïve $CD4^+$ T cells and induce the Th1/Th2/Treg imbalance in the intestinal immune response. This imbalance will contribute to the opposite directions of the susceptibility to UC and CD. Further studies to clarify the mechanisms of this HLA haplotype on the homeostasis of the intestinal immune system are needed.

Clinical importance of differential diagnosis of UC and CD has been recognized, and incorporation of genetic markers in the diagnosis is proposed as a promising clue.[44,45] The identified HLA haplotype distinguishes UC and CD with OR of as large as around 6.5, which would have more impacts than the previously evaluated variants.[45] Thus, utilization of the genotype information of the HLA haplotype, or alternatively the SNP(s) in LD with it, might contribute to improvements of diagnostic approaches on UC and CD.

In summary, our study demonstrated that the particular HLA haplotype has the opposite directions of genetic effects on UC and CD. Our findings should shed light on the pathogenesis of IBD.

Supplementary Material

Note: To access the supplementary material accompanying this article, visit the online version of *Gastroenterology* at www.gastrojournal.org, and at doi: 10.1053/j.gastro.2011.05.048.

References

1. Podolsky DK. Inflammatory bowel disease. N Engl J Med 2002; 347:417–429.
2. Cho JH. The genetics and immunopathogenesis of inflammatory bowel disease. Nat Rev Immunol 2008;8:458–466.
3. Bouma G, Strober W. The immunological and genetic basis of inflammatory bowel disease. Nat Rev Immunol 2003;3:521–533.
4. Yamazaki K, McGovern D, Ragoussis J, et al. Single nucleotide polymorphisms in TNFSF15 confer susceptibility to Crohn's disease. Hum Mol Genet 2005;14:3499–3506.
5. Duerr RH, Taylor KD, Brant SR, et al. A genome-wide association study identifies IL23R as an inflammatory bowel disease gene. Science 2006;314:1461–1463.
6. Hampe J, Franke A, Rosenstiel P, et al. A genome-wide association scan of nonsynonymous SNPs identifies a susceptibility variant for Crohn disease in ATG16L1. Nat Genet 2007;39:207–211.
7. Rioux JD, Xavier RJ, Taylor KD, et al. Genome-wide association study identifies new susceptibility loci for Crohn disease and implicates autophagy in disease pathogenesis. Nat Genet 2007; 39:596–604.
8. Libioulle C, Louis E, Hansoul S, et al. Novel Crohn disease locus identified by genome-wide association maps to a gene desert on 5p13.1 and modulates expression of PTGER4. PLoS Genet 2007; 3:e58.
9. Parkes M, Barrett JC, Prescott NJ, et al. Sequence variants in the autophagy gene IRGM and multiple other replicating loci contribute to Crohn's disease susceptibility. Nat Genet 2007;39:830–832.
10. The WTCCC. Genome-wide association study of 14,000 cases of seven common diseases and 3,000 shared controls. Nature 2007;447:661–678.

11. Raelson JV, Little RD, Ruether A, et al. Genome-wide association study for Crohn's disease in the Quebec Founder Population identifies multiple validated disease loci. Proc Natl Acad Sci U S A 2007;104:14747–14752.
12. Barrett JC, Hansoul S, Nicolae DL, et al. Genome-wide association defines more than 30 distinct susceptibility loci for Crohn's disease. Nat Genet 2008;40:955–962.
13. Franke A, Balschun T, Karlsen TH, et al. Sequence variants in IL10, ARPC2 and multiple other loci contribute to ulcerative colitis susceptibility. Nat Genet 2008;40:1319–1323.
14. Silverberg MS, Cho JH, Rioux JD, et al. Ulcerative colitis-risk loci on chromosomes 1p36 and 12q15 found by genome-wide association study. Nat Genet 2009;41:216–220.
15. Asano K, Matsushita T, Umeno J, et al. A genome-wide association study identifies three new susceptibility loci for ulcerative colitis in the Japanese population. Nat Genet 2009;41:1325–1329.
16. McGovern DP, Gardet A, Torkvist L, et al. Genome-wide association identifies multiple ulcerative colitis susceptibility loci. Nat Genet 2010;42:332–337.
17. Franke A, Balschun T, Sina C, et al. Genome-wide association study for ulcerative colitis identifies risk loci at 7q22 and 22q13 (IL17REL). Nat Genet 2010;42:292–294.
18. Fisher SA, Tremelling M, Anderson CA, et al. Genetic determinants of ulcerative colitis include the ECM1 locus and five loci implicated in Crohn's disease. Nat Genet 2008;40:710–712.
19. Franke A, Balschun T, Karlsen TH, et al. Replication of signals from recent studies of Crohn's disease identifies previously unknown disease loci for ulcerative colitis. Nat Genet 2008;40:713–715.
20. Anderson CA, Massey DC, Barrett JC, et al. Investigation of Crohn's disease risk loci in ulcerative colitis further defines their molecular relationship. Gastroenterology 2009;136:5239.e3.
21. Wang K, Baldassano R, Zhang H, et al. Comparative genetic analysis of inflammatory bowel disease and type 1 diabetes implicates multiple loci with opposite effects. Hum Mol Genet 2010;19:2059–2067.
22. Futami S, Aoyama N, Honsako Y, et al. HLA-DRB1*1502 allele, subtype of DR15, is associated with susceptibility to ulcerative colitis and its progression. Dig Dis Sci 1995;40:814–818.
23. Stokkers PC, Reitsma PH, Tytgat GN, et al. HLA-DR and -DQ phenotypes in inflammatory bowel disease: a meta-analysis. Gut 1999;45:395–401.
24. Ahmad T, Marshall SE, Jewell D. Genetics of inflammatory bowel disease: the role of the HLA complex. World J Gastroenterol 2006;12:3628–3635.
25. Rioux JD, Goyette P, Vyse TJ, et al. Mapping of multiple susceptibility variants within the MHC region for 7 immune-mediated diseases. Proc Natl Acad Sci U S A 2009;106:18680–18685.
26. Lennard-Jones JE. Classification of inflammatory bowel disease. Scand J Gastroenterol Suppl 1989;170:2–6.
27. Yamazaki K, Onouchi Y, Takazoe M, et al. Association analysis of genetic variants in IL23R, ATG16L1 and 5p13.1 loci with Crohn's disease in Japanese patients. J Hum Genet 2007;52:575–583.
28. Purcell S, Neale B, Todd-Brown K, et al. PLINK: a tool set for whole-genome association and population-based linkage analyses. Am J Hum Genet 2007;81:559–575.
29. The International HapMap Consortium. The International HapMap Project. Nature 2003;426:789–796.
30. Price AL, Patterson NJ, Plenge RM, et al. Principal components analysis corrects for stratification in genome-wide association studies. Nat Genet 2006;38:904–909.
31. Barrett JC, Fry B, Maller J, et al. Haploview: analysis and visualization of LD and haplotype maps. Bioinformatics 2005;21:263–265.
32. Kumasaka N, Nakamura Y, Kamatani N. The textile plot: a new linkage disequilibrium display of multiple-single nucleotide polymorphism genotype data. PLoS One 2010;5:e10207.
33. Lake SL, Lyon H, Tantisira K, et al. Estimation and tests of haplotype-environment interaction when linkage phase is ambiguous. Hum Hered 2003;55:56–65.
34. Northridge ME. Public health methods—attributable risk as a link between causality and public health action. Am J Public Health 1995;85:1202–1204.
35. Yamaguchi-Kabata Y, Nakazono K, Takahashi A, et al. Japanese population structure, based on SNP genotypes from 7003 individuals compared to other ethnic groups: effects on population-based association studies. Am J Hum Genet 2008;83:445–456.
36. de Bakker PI, McVean G, Sabeti PC, et al. A high-resolution HLA and SNP haplotype map for disease association studies in the extended human MHC. Nat Genet 2006;38:1166–1172.
37. Okada Y, Yamada R, Suzuki A, et al. Contribution of a haplotype in the HLA region to anti-cyclic citrullinated peptide antibody positivity in rheumatoid arthritis, independently of HLA-DRB1. Arthritis Rheum 2009;60:3582–3590.
38. Abraham C, Cho JH. Inflammatory bowel disease. N Engl J Med 2009;361:2066–2078.
39. Kugathasan S, Baldassano RN, Bradfield JP, et al. Loci on 20q13 and 21q22 are associated with pediatric-onset inflammatory bowel disease. Nat Genet 2008;40:1211–1215.
40. Round JL, Mazmanian SK. The gut microbiota shapes intestinal immune responses during health and disease. Nat Rev Immunol 2009;9:313–323.
41. Medzhitov R. Recognition of microorganisms and activation of the immune response. Nature 2007;449:819–826.
42. Steinman L. A brief history of T(H)17, the first major revision in the T(H)1/T(H)2 hypothesis of T cell-mediated tissue damage. Nat Med 2007;13:139–145.
43. Bedoui S, Kupz A, Wijburg OL, et al. Different bacterial pathogens, different strategies, yet the aim is the same: evasion of intestinal dendritic cell recognition. J Immunol 2010;184:2237–2242.
44. Geboes K, Colombel JF, Greenstein A, et al. Indeterminate colitis: a review of the concept—what's in a name? Inflamm Bowel Dis 2008;14:850–857.
45. Vermeire S, Van Assche G, Rutgeerts P. Role of genetics in prediction of disease course and response to therapy. World J Gastroenterol 2010;16:2609–2615.

Received December 27, 2010. Accepted May 26, 2011.

Reprint requests

Address requests for reprints to: Michiaki Kubo, MD, PhD, Laboratory for Genotyping Development, Center for Genomic Medicine, RIKEN Yokohama Institute, 1-7-22 Suehiro-cho, Tsurumi-ku, Yokohama, Kanagawa, 230-0045, Japan. e-mail: mkubo@src.riken.jp; phone: +81-45-503-9607; fax: +81-45-503-9606.

Acknowledgments

We are grateful to the members of the Rotary Club of Osaka-Midosuji District 2660 Rotary International in Japan for supporting our study. We thank all the staffs of Laboratory for Genotyping Development, Center for Genomic Medicine, RIKEN for their contribution to SNP genotyping.

Conflicts of interest

The authors disclose no conflicts.

Funding

This work was supported by the Ministry of Education, Culture, Sports, Sciences and Technology of the Japanese government.

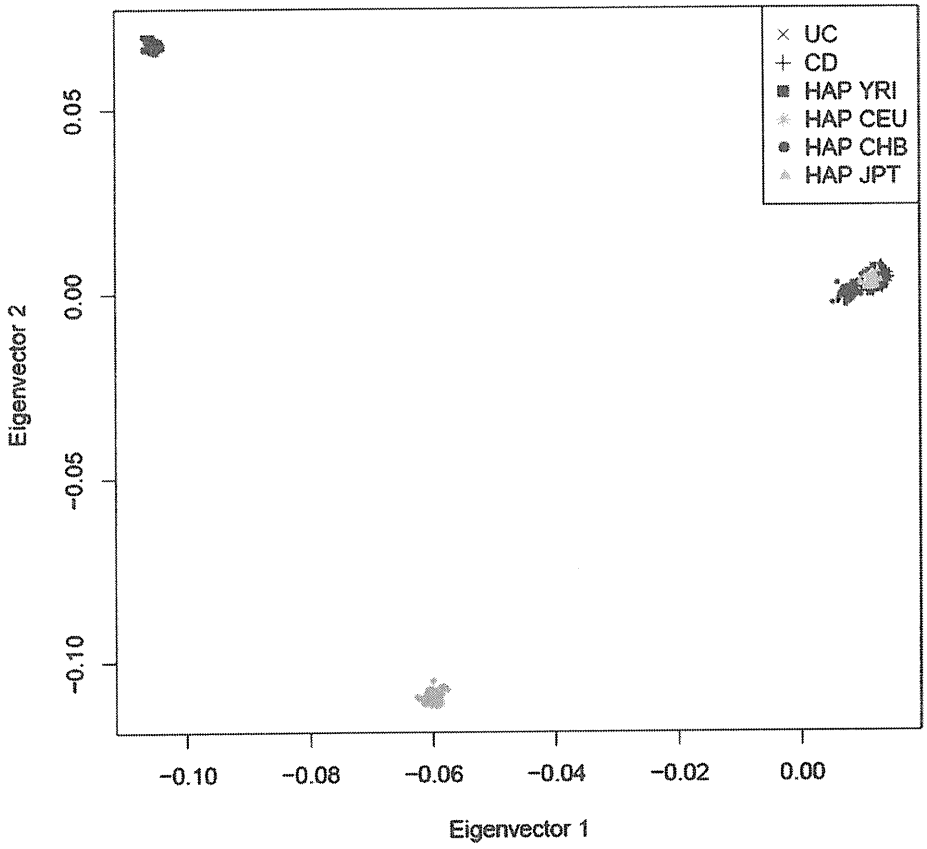

Supplementary Figure 1. Principal component analysis (PCA) plot of the subjects. UC cases and CD cases enrolled in the GWAS are plotted based on eigenvectors 1 and 2 obtained from the PCA using EIGENSTRAT, along with the European (CEU), African (YRI), Japanese (JPT), and Chinese (CHB) individuals obtained from the Phase II HapMap database (release 22).

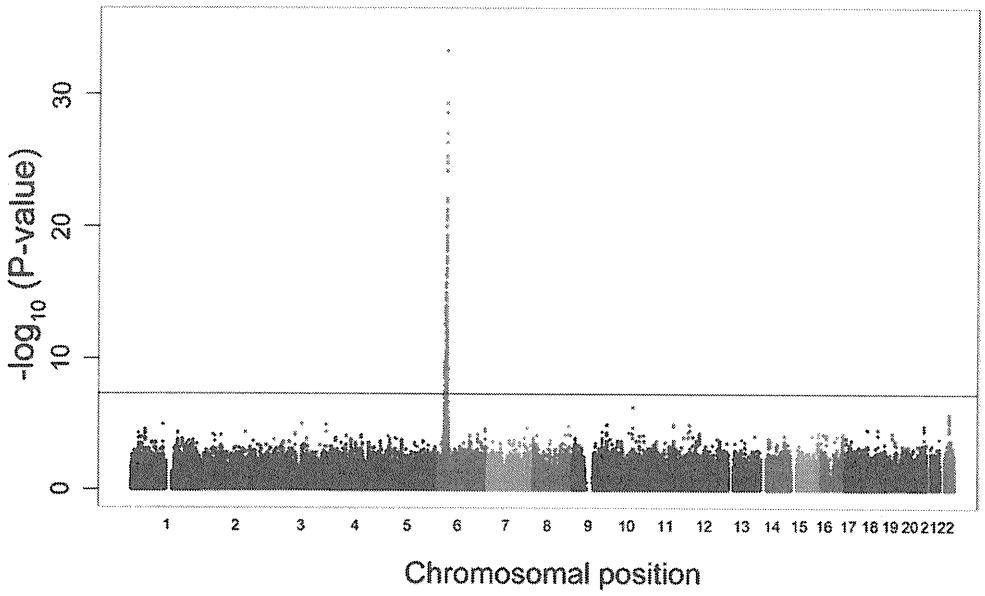

Supplementary Figure 2. Manhattan plot of the comparative GWAS using 372 UC cases and 372 CD cases. The *gray horizontal lines* in the plots represent the genome-wide significance threshold of $P = 5.0 \times 10^{-8}$.